A&A 579, A121 (2015)
DOI: 10.1051/0004-6361/201526518

Astronomy & Astrophysics

New constraints on the CH_4 vertical profile in Uranus and Neptune from *Herschel* observations⋆

E. Lellouch[1], R. Moreno[1], G. S. Orton[2], H. Feuchtgruber[3], T. Cavalié[4], J. I. Moses[5], P. Hartogh[4], C. Jarchow[4], and H. Sagawa[6]

[1] LESIA, Observatoire de Paris, 5 place Jules Janssen, 92195 Meudon, France
e-mail: emmanuel.lellouch@obspm.fr
[2] Jet Propulsion Laboratory, California Institute of Technology, 4800 Oak Grove Drive Pasadena, CA 91109, USA
[3] Max-Planck-Institut für Extraterrestrische Physik, Giessenbachstraße, 85748 Garching, Germany
[4] Max-Planck-Institut für Sonnensystemforschung, Justus-von-Liebig-Weg 3, 37077 Göttingen, Germany
[5] Space Science Institute, 4750 Walnut St., Suite 205, Boulder, CO 80301, USA
[6] Faculty of Science, Kyoto Sangyo University. Motoyama, Kamigamo, Kita-ku, Kyoto 603-8555, Japan

Received 12 May 2015 / Accepted 12 June 2015

ABSTRACT

Dedicated line observations of CH_4 rotational lines performed with *Herschel*/PACS and HIFI in 2009–2011 provide new inferences of the mean methane profile in the upper tropospheres and stratospheres of Uranus and Neptune. At Uranus, CH_4 is found to be near saturation, with a $\sim 9 \times 10^{-4}$ tropopause/lower stratosphere mole fraction. This is nominally six times larger than inferred from *Spitzer* in 2007, although reconciliation may be possible if the CH_4 abundance decreases sharply from ~100 to 2 mbar. This unexpected situation might reflect heterogeneous conditions in Uranus' stratosphere, with local CH_4 depletions and heating associated with downwelling motions. Higher CH_4 abundances compared to values inferred under solstitial conditions by Voyager in 1989 suggest that atmospheric mixing is effectively subdued at high latitudes and/or is time-variable. At Neptune, the mid-stratosphere CH_4 abundance is $(1.15 \pm 0.10) \times 10^{-3}$, in agreement with earlier determinations and indicative of either leakage through a warmer polar region or upwelling at low or middle latitudes. On both planets, spatially resolved observations of temperature and methane in the stratosphere are needed to further identify the physical processes at work.

Key words. planetary systems – planets and satellites: gaseous planets – planets and satellites: individual: Uranus – planets and satellites: individual: Neptune

1. Introduction

Methane is the third most abundant species in the observable atmosphere of the giant planets and the starting point of hydrocarbon photochemistry. In Uranus and Neptune, the methane deep abundance is large (several percent), but condensation in the upper troposphere reduces the amount of stratospheric CH_4 available to photolysis to much lower values, and a further limitation in Uranus is associated with the low (~0.05 mbar) homopause. In a simplistic view, CH_4 would be vertically and horizontally uniform up to its condensation level near 1.5 bar, then follow a saturation profile up to the tropopause, thereby determining its stratospheric abundance. Previous observations at a variety of wavelengths have revealed a more complex picture. Despite nearly identical globally averaged tropopause temperatures, stratospheric CH_4 is strongly enhanced in Neptune vs. Uranus (Baines & Hammel 1994). Furthermore, both planets exhibit nonuniformly mixed, subsaturated, and latitudinally variable CH_4 profiles below the 1.5 bar level (Karkoschka & Tomasko 2011; Sromovsky et al. 2014). These findings indicate that non-1D and presumably seasonally variable processes are at work, such as upwelling and downwelling convective cells transporting CH_4-rich or depleted air, or "leakage" of CH_4 gas into the stratosphere from locally warm regions.

The operation of *Herschel* (Pilbratt et al. 2010) in 2009–2013 offered an opportunity to measure the CH_4 abundance in a new range (far-IR/submm) that has several advantanges, such as (i) the weak dependence of the emitted radiation with temperature; (ii) the absence of scattering effects that affect short-wavelength observations; and (iii) the possibility to spectrally resolve individual lines, using heterodyne spectroscopy. Although Uranus and Neptune were not spatially resolved by *Herschel*, these measurements provide a characterization of the mean CH_4 vertical profile in these bodies and the associated physics and establish a benchmark for seasonal variability studies.

2. CH_4 observations

Scientific observations of Uranus and Neptune by *Herschel* consisted of a combination of full-range spectroscopy with the Photoconductor Array Camera and Spectrometer (PACS, Poglitsch et al. 2010) and the Spectral and Photometric Imaging Receiver (SPIRE, Griffin et al. 2010), mostly acquired within the *Herschel* solar system observations (HssO, KPGTpharto01_1) guaranteed time key program (Hartogh et al. 2009), and targeted line observations with PACS and the *Herschel* Heterodyne Instrument for the Far-Infrared (HIFI,

⋆ *Herschel* is an ESA space observatory with science instruments provided by European-led Principal Investigator consortia and with important participation from NASA.

Table 1. Summary of observations.

Object	Obs. ID	Program	Instrument/Mode	Start time [UTC]	T_{obs} [min]	Range	Resolving power
Uranus	1342199899	KPGTpharto01_1	PACSLineSpec	2010-07-06 10:26	111	118.4–121.0 μm	1050
Uranus	1342199890	KPGTpharto01_1	PACSLineSpec	2010-07-06 12:19	111	158.1–160.3 μm	1300
Uranus	1342237588	OT1_rmoreno_2	PACSLineSpec	2012-01-17 10:29	614	158.3–160.3 μm	1300
Neptune	1342186539	OT1_rmoreno_2	PACSRangeSpec	2009-10-30 08:53	151	120–171 μm	1300
Neptune	1342186571	KPGTpharto01_1	PACSLineSpec	2009-10-31 14:35	82	118.4–120.9 μm	1050
Neptune	1342233296	OT1_rmoreno_2	HIFIPoint	2011-11-29 06:32	421	1881.6–1883.4 GHz	10^6

de Graauw et al. 2010) for some species of interest (e.g., H_2O, CO, CH_4), acquired both within HssO and open time (OT) programs – see, for instance, Cavalié et al. (2014). Dedicated observations of CH_4 targeted the J = 6–5 and J = 8–7 multiplets at 159.3 and 119.6 μm, respectively. Early PACS observations of Neptune within HssO provided easy detections of the CH_4 lines (Lellouch et al. 2010), warranting a more detailed, spectrally resolved investigation with HIFI. At Uranus, in contrast, initial PACS observations of J = 6–5 and J = 8–7 led to only marginal detections, requiring much deeper integrations. These follow-up observations of CH_4 with HIFI at Neptune and PACS at Uranus were obtained within the OT1_rmoreno_2 program, targeting in both cases the J = 6–5 multiplet. Observational details of all the targeted observations are given in Table 1.

PACS observations were carried out in chopped-nodded line spectroscopy modes. They were processed by standard PACS pipeline modules up to Level 1. Additional steps in the data reduction included the removal of signal outliers on the individual spectra pixels and the rebinning of data on an oversampled wavelength grid (see details, e.g., in Lellouch et al. 2010). Given the apparent sizes of about 3.5″ (Uranus) and 2.3″ (Neptune), only the 9.4″ × 9.4″ central PACS spaxel was considered, and the spectra were divided by their local continuum, removing absolute flux calibration uncertainties.

HIFI observations of Neptune were conducted in position-switch mode. They covered the 1881.6–1883.4 GHz range, which includes several components of the CH_4 J = 6–5 multiplet. As for PACS, the HIFI beam (11.2″ at 1882 GHz) entirely encompassed Neptune. The spectral resolution was 1.1 MHz (Wide Band Spectrometer), but since lines are smeared by the planet rotation (equatorial velocity =2.66 km s^{-1}), data were smoothed to $\Delta\nu$ = 12 MHz (i.e., 1.9 km s^{-1} at 1882 GHz) to enhance the signal-to-noise ratio (S/N). Data reduction was carried out using the *Herschel* data reduction software HIPE, version 8.1 (Ott 2010). Additional baseline removal (simple sine function) was applied. Data were also expressed in line-to-continuum ratios to eliminate the effect of pointing and beam efficiency uncertainties.

3. Modeling and results

Observations were analyzed by means of standard radiative transfer codes (Lellouch et al. 2010; Moreno et al. 2012; Orton et al. 2014a), in which the outgoing radiance was integrated over all emission angles, including H_2-He-CH_4 collision-induced absorption (CIA; see, e.g., details in Orton et al. 2014a), and the CH_4 line opacity based on spectroscopic parameters from Boudon et al. (2010). The CO line opacity was included for Neptune.

3.1. Uranus

Orton et al. (2014a,b) used a high-quality *Spitzer* IRS spectrum to obtain the most recent and detailed characterization of Uranus' mean thermal structure and composition. The thermal structure, which we adopt here, was determined by the requirement to match the 9–20 μm CIA continuum, as well as the H_2 S(1)-S(4) quadrupole lines. We note that the associated continuum model is also consistent, to within ±3% at most, with *Herschel* SPIRE spectroscopy over 200–670 μm (itself calibrated on Mars Swinyard et al. 2014). The 7.4–9.5 μm range was then used to determine the CH_4 vertical profile, described by physics-based diffusion models in which free parameters are the tropopause CH_4 mole fraction (f_{CH_4}) and the stratospheric eddy diffusion coefficient (K_{zz}), which was assumed to be constant with altitude. The best fit was obtained for $f_{CH_4} = (1.6^{+0.2}_{-0.1}) \times 10^{-5}$ (corresponding to 23% relative humidity (RH)) and $K_{zz} = 2430^{+100}_{-190}$ cm^2 s^{-1}. In the troposphere, the CH_4 profile smoothly joins to a deep mole fraction that is assumed to be 3.2%, following Karkoschka & Tomasko (2009), at some adjustable pressure that is found to be equal to 1.78 ± 0.20 bar for the best fit.

The spectrally resolved *Herschel*/PACS spectrum provides independent constraints on the CH_4 profile. First, the lack of emission in the core of the 159.3 μm multiplet implies a sharp decrease of CH_4 at pressures lower than ∼1 mbar, associated with the low homopause. Second, the depth and width of the absorption feature determine the CH_4 mole fraction to be about 1×10^{-4} near the 200 mbar level – inconsistent with the *Spitzer*-preferred profile (Fig. 1). Orton et al. (2014b) proposed additional solution fits invoking lower K_{zz} and higher f_{CH4} values. Continuing with this sort of models, the PACS line can be fit with K_{zz} = 1020 cm^2 s^{-1} and $f_{CH_4} = 9.2 \times 10^{-5}$. However, this solution implies 115% CH_4 global humidity at the tropopause and overpredicts the 7.7 μm emission in the IRS data (Fig. 3). We constructed an empirical CH_4 profile by smoothly decreasing the RH from the saturation level to a pressure of 800 mbar, with a constant RH between 800 mbar and 100 mbar, and a constant log-log slope with pressure above the 100-mbar level. A good fit of both the PACS and IRS spectra (Figs. 2 and 3) was obtained for a 75% RH over 100–800 mbar, indicating a 4.7×10^{-5} mole fraction at the 89 mbar temperature minimum (T = 52.4 K), smoothly joining to 1.6×10^{-5} at 2.5 mbar (Fig. 1). Weighting functions (WF) calculated for this best fit profile, in the CH_4 line core (159.3 μm) and wing (159.0 μm) and convolved to PACS resolution, are shown in Fig. 1, after subtraction of the continuum WF. They illustrate that the CH_4 line mostly probes the 0.1–0.6 bar range. The fit of the PACS spectrum is thus not particularly sensitive to the CH_4 slope in the stratosphere, but the latter permits maintaining a good fit of the *Spitzer* 7.4–9.5 μm range (Fig. 3). As discussed below, this empirical profile is unlikely

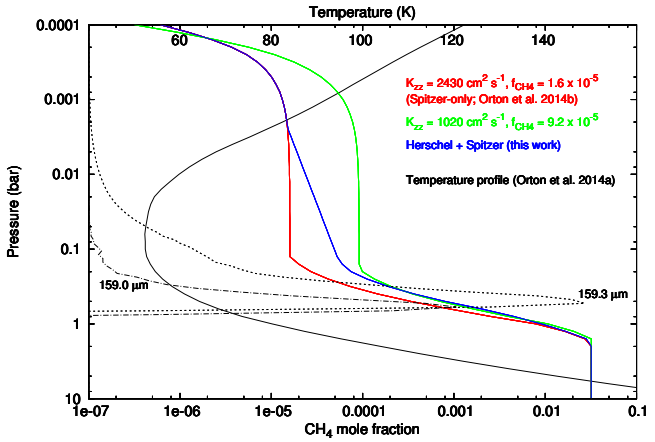

Fig. 1. Temperature (solid black line) and CH_4 profiles in Uranus. Red and green profiles are based on diffusion models. The blue curve is the empirical profile that simultaneously matches *Herschel*/PACS and *Spitzer*/IRS (see text). The thin dotted (dashed-dotted) line shows weighting functions in the core – 159.3 μm (wing – 159.0 μm) of the CH_4 line at PACS resolution, calculated for this solution profile. The *Spitzer*/IRS spectrum (Fig. 3) also constrains the CH_4 profile in the region of ~0.1 mbar.

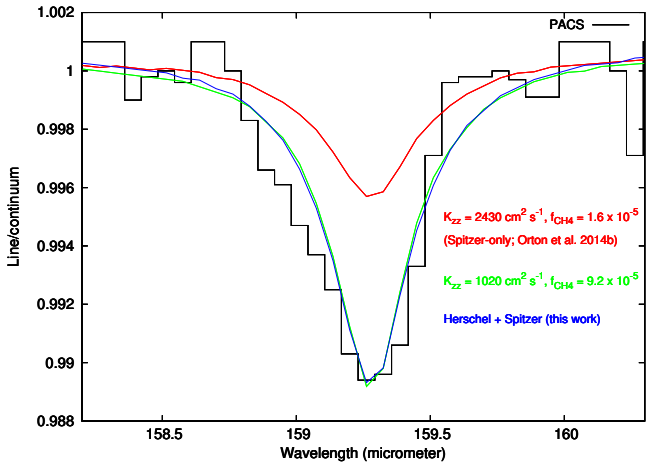

Fig. 2. CH_4 J = 6–5 multiplet at Uranus, observed with PACS. The spectral resolution is $\delta\lambda$ = 0.12 μm ($\lambda/\delta\lambda$ ~1300). Observations are compared to models with the three CH_4 distributions shown in Fig. 1.

to represent the actual methane profile at all locations in the stratosphere of Uranus, and instead probably reflects the interplay of spatial heterogeneities in stratospheric temperatures and methane abundances.

3.2. Neptune

Previous analyses of the Neptune PACS spectrum (Lellouch et al. 2010; Feuchtgruber et al. 2013) have made use of thermal profiles from earlier work, tuned to match the appearance of the R(0) and R(1) HD lines detected in that spectrum (Feuchtgruber et al. 2013 also included the HD R(2) line measured by ISO). These profiles were however not consistent with each other (with, e.g., a ~4 K difference at the tropopause). Here, we used a temperature profile (Fig. 4) constrained by a broader combination of data, including the SPIRE 200–670 μm spectrum, the ISO continuum (Burgdorf et al. 2003), ground-based measurements over 17–23 μm (Orton et al. 1992), and the PACS HD lines, adopting the profile reported by Fletcher et al. (2010) in the

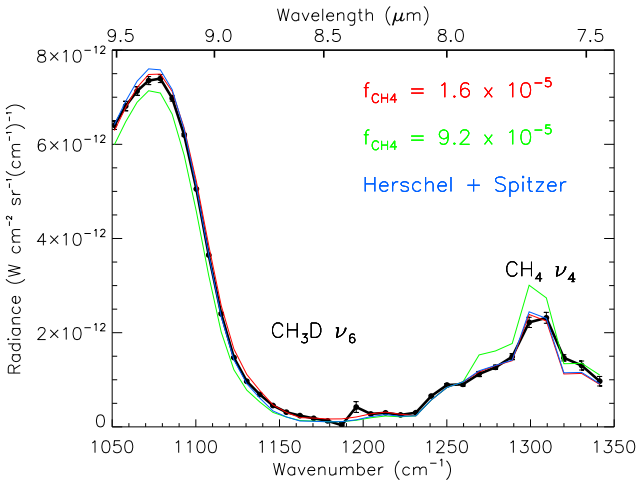

Fig. 3. *Spitzer* spectrum of Uranus in the 1050–1350 cm^{-1} (7.4–9.5 μm) range from Orton et al. (2014b), compared to models with the CH_4 distributions of Fig. 1 (same color codes are used).

stratosphere at p < 1 mbar. Our P(T) profile is identical to that of Lellouch et al. (2010) at p > 300 mbar, and 1–2 K colder over 3–100 mbar. On the other hand, it is significantly warmer (by 3–4 K at all levels) than the profile obtained by Feuchtgruber et al. (2013). The near-tropopause (100 mbar) temperature is 53.5 K, slightly lower than determined by Fletcher et al. (2014) from various imaging and spectroscopic datasets over 2003–2007. We note that our adopted profile also permits a fit to the CO lines in SPIRE and ground-based observations with broad bandwidth (Moreno et al., in prep.).

The HIFI observations (Fig. 4) spectrally separate and resolve the J = 6–5 multiplet into four individual emission features, which altogether constrain the CH_4 vertical profile over 0.5–30 mbar. PACS observations of the same line extend the probed region down to the tropopause, and the lack of absorption in this line (Lellouch et al. 2010) precludes CH_4 from being uniform in the lower stratosphere. The best-fit CH_4 profile (Fig. 4) has a (1.15 ± 0.10) × 10^{-3} mixing ratio at 20 mbar and above, decreasing toward the tropopause according to local saturation. The upper stratospheric mixing ratio appears intermediate between previous determinations from Akari – (0.9 ± 0.2) × 10^{-3} (Fletcher et al. 2010) and the early PACS-derived abundance – (1.5 ± 0.2) × 10^{-3} (Lellouch et al. 2010). Consistency with *Spitzer*/IRS data is deferred to future work, after those data are published on their own.

4. Discussion

Uranus. Based on HST/STIS observations of Uranus, Karkoschka & Tomasko (2009) found unexpected latitudinal variations of tropospheric CH_4, which they interpreted as being due to variations of the "deep" (1–3 bar) CH_4 mole fraction (from 0.014 to 0.032), with a common profile above the one-bar level, having ~48% RH near 1 bar and about five times less at the tropopause. In an updated interpretation (Karkoschka & Tomasko 2011), methane profiles were described with a variable latitude slope over 1–3 bar (see their Fig. 10). The best-fit profile from *Spitzer*/IRS (Orton et al. 2014b) was similar to the Karkoschka & Tomasko (2011) profile at 33°S. In contrast, PACS observations imply that the atmosphere of Uranus is significantly more rich in methane at altitudes above the one-bar level. More specifically, the PACS spectrum can be fit with f_{CH_4} = 9.2 × 10^{-5} at the tropopause,

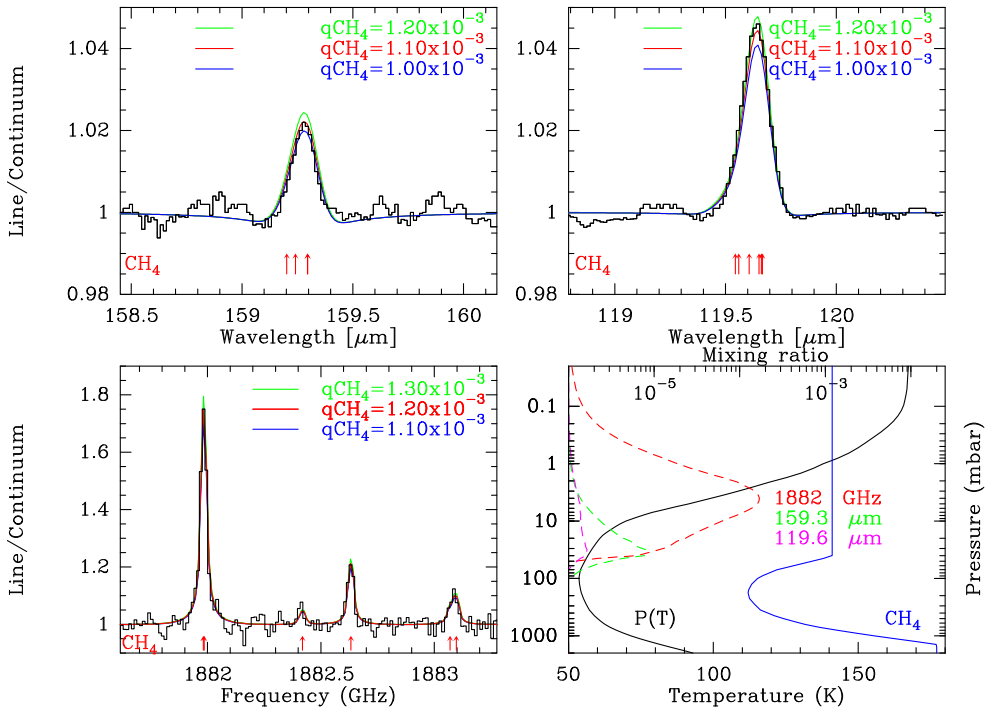

Fig. 4. PACS (*top*) and HIFI (*bottom left*) observations of Neptune compared to models with varying mid-stratospheric CH_4 mixing ratios. *Bottom right panel*: atmospheric model. Solid lines: temperature (black) and CH_4 (blue) profiles. Dashed lines: contribution functions for the CH_4 J = 6–5 1882.0 GHz line (at HIFI resolution) and for the J = 6–5 (159.3 μm) and J = 8–7 (119.6 μm) multiplets (at PACS resolution).

corresponding to 115% RH for the global average temperature profile. This is inconsistent with inferences at the Voyager 2 radio-occultation locations (Lindal et al. 1987; Sromovsky et al. 2011), which do not indicate tropopause CH_4 mole fractions anywhere near saturation. We note, however, that a factor-of-1.15 supersaturation is equivalent to a temperature difference of only ~0.4 K, so that mild spatial temperature heterogeneities and/or convective overshooting from upwelling regions could explain the elevated CH_4 mole fractions. Such a profile still overpredicts the *Spitzer*/IRS-measured 7.7 μm CH_4 emission (Fig. 3). Reconciliation (and alleviation of the supersaturation) can be achieved by invoking a CH_4 profile that declines by a factor of five from 100 to 2 mbar, but at least in a 1D description, such a non-uniform profile is not expected in a region dominated by eddy transport and where no effective chemical loss is at work. A possibility is that the apparent CH_4 vertical profile reflects spatial heterogeneities in stratospheric temperatures and methane abundance, bearing in mind that the short-wavelength *Spitzer* data are more heavily weighted toward warmer regions of the planet (while the *Herschel* data probe more globally averaged conditions). In the simple picture where the CH_4 stratospheric abundance is determined by the cold trap temperature, it may seem counter-intuitive to associate these warmer regions with *lower* CH_4 amounts. However, warm regions may be caused by local adiabatic heating due to localized downwelling motions. By effectively acting against the mixing from below, these vertical winds would locally decrease the CH_4 stratospheric amounts, possibly leading to non-uniform profiles similar to the one we infer. These downward winds would also tend to smooth out the positive vertical gradients of the hydrocarbon profiles. These possibilities cannot be verified for the time being because we lack spatially resolved measurements of the thermal emission field from Uranus. Future observations, in particular from JWST/MIRI thermal spectro-imaging data, are expected to shed light on these scenarios.

The recent observations from *Spitzer* and *Herschel* sample near-equinoctial conditions (subsolar latitude $\beta \sim 0°$ in 2007 and $\beta \sim +15°$ in 2011), in contrast with the epochs of Voyager ($\beta \sim -80°$ in 1986) and ISO ($\beta \sim -40°$ in 1997). Our CH_4 stratospheric abundance exceeds the values or upper limits inferred from Voyager, especially at high latitudes (Yelle et al. 1989), while being reasonably consistent with the upper limit from ISO (Encrenaz et al. 1998). This supports the view (Yelle et al. 1989; Moses 2008; Orton et al. 2014b, and references therein) that vertical transport depends on latitude, with global circulation effectively decreasing the strength of atmospheric mixing in the stratosphere at high latitudes. This picture could be consistent with the decrease of the upper tropospheric methane from equator to pole (Karkoschka & Tomasko 2009; Sromovsky et al. 2014), possibly caused by upward transport of CH_4-rich air at low latitudes and downward motion of CH_4-dessicated air over the poles, provided that these cells extend into the stratosphere. Time variability of the convective activity, being more developed near Equinox, is also possible and is supported by the surge of cloud activity near equinox – except at high southern latitudes (Sromovsky et al. 2012).

Neptune. At Neptune, the mid-stratosphere methane mixing ratio is about eight times greater than allowed by the mean 56 K cold trap, but otherwise follows saturation at the local temperature over 20–100 mbar. The enhanced (~0.0012) CH_4 mixing ratio, consistent with saturation at ~59 K, may be due to (i) "leakage" through a warm tropopause at high southern latitudes, where temperatures of 62–66 K have been observed in 2003 (Orton et al. 2007); (ii) upwelling and/or convective overshooting, at either equatorial (Karkoschka & Tomasko 2011) or middle latitudes (de Pater et al. 2014). Based on multiwavelength observations and extending over scenarios by Bézard et al. (1991) and Conrath et al. (1991), de Pater et al. (2014) and Fletcher et al. (2014) proposed a hemispherically symmetric circulation pattern covering a very broad (>10-bar to <1 mbar) vertical range,

with rising (and cooling) air at mid-latitudes and subsidence over the poles and equator. If true, this scenario, might argue against the "polar leakage" hypothesis. We note, however, that it does not seem consistent with the equator-to-pole decrease in the CH_4 tropospheric abundance (Karkoschka & Tomasko 2011). Furthermore, the consistency of the CH_4 stratospheric profile with local saturation may instead favor the leakage idea, as one might expect dynamical scenarios to lead to a vertically more uniform (or uncorrelated with temperature) abundance profile. An important missing piece to the puzzle – also needed to interpret the surprisingly latitudinally uniform stratospheric emission from Neptune (Greathouse et al. 2011; Fletcher et al. 2014) – is the latitudinal distribution of stratospheric CH_4 and its putative correlation with the temperature field.

Acknowledgements. HIFI has been designed and built by a consortium of institutes and university departments from across Europe, Canada, and the United States under the leadership of SRON Netherlands Institute for Space Research, Groningen, The Netherlands, and with major contributions from Germany, France, and the US. Consortium members are: Canada: CSA, U. Waterloo; France: CESR, LAB, LERMA, IRAM; Germany: KOSMA, MPIfR, MPS; Ireland, NUI Maynooth; Italy: ASI, IFS I-INAF, Osservatorio Astrofisico di Arcetri-INAF; Netherlands: SRON, TUD; Poland: CAMK, CBK; Spain: Observatorio Astronómico Naci onal (IGN), Centro de Astrobiología (CSIC-INTA). Sweden: Chalmers University of Technology – MC2, RSS & GARD; Onsala Space Observatory; Swedish National Space Board, Stockholm University – Stockholm Observatory; Switzerland: ETH Zurich, FHNW; USA: Caltech, JPL, NHSC. PACS has been developed by a consortium of institutes led by MPE (Germany) and including UVIE (Austria); KUL, CSL, IMEC (Belgium); CEA, OAMP (France); MPIA (Germany); IFSI, OAP/AOT, OAA/CAISMI, LENS, SISSA (Italy); IAC (Spain). This development has been supported by the funding agencies BMVIT (Austria), ESA-PRODEX (Belgium), CEA/CNES (France), DLR (Germany), ASI (Italy), and CICT/MCT (Spain). Additional funding support for some instrument activities has been provided by ESA. Data presented in this paper were analysed using "HIPE", a joint development by the *Herschel* Science Ground Segment Consortium, consisting of ESA, the NASA *Herschel* Science Center, and the HIFI, PACS and SPIRE consortia.

References

Baines, K., & Hammel, H. 1994, Icarus, 109, 20
Bézard, B., Romani, P., Conrath, B. J., & Maguire, W. C. 1991, J. Geophys. Res., 96, 18961
Conrath, B., Flasar, F. M., & Gierasch, P. J. 1991, J. Geophys. Res., 96, 18931
Boudon, V., Pirali, O., Roy, P., et al. 2010, J. Quant. Spectro. Rad. Transf., 111, 1117
Burgdorf, M., Orton, G. S., Davis, G. R., et al. 2003, Icarus, 164, 244
Cavalié, T., Moreno, R., Lellouch, E., et al. 2014, A&A, 562, A33
de Graauw, T., Helmich, F. P., Phillips, T. G., et al. 2010, A&A, 518, L6
de Pater, I., Fletcher, L. N., Luszcz-Cook, S., et al. 2014, Icarus, 237, 211
Encrenaz, T., Feuchtgruber, H., Atreya, S. K., et al. 1998, A&A, 333, L43
Feuchtgruber, H., Lellouch, E., Orton, E. et al. 2013, A&A, 551, A126
Fletcher, L. N., Drossart, P., Burgdorf, M., et al. 2010, A&A, 514, A17
Fletcher, L. N., De Pater, I., Orton, G. S., et al. 2014, Icarus, 231, 146
Greathouse, T. K., Richter, M., Lacy, J., et al. 2011, Icarus, 214, 606
Griffin, M., Abergel, A., Abreu, A., et al. 2010, A&A, 518, L3
Hartogh, P., Lellouch, E., Crovisier, J., et al. 2009, Planet. Space Sci., 57, 1596
Karkoschka, E., & Tomasko, M. E. 2009, Icarus, 202, 287
Karkoschka, E., & Tomasko, M. E. 2011, Icarus, 211, 780
Lellouch, E., Hartogh, P., Feuchtgruber, H., et al. 2010, A&A, 518, L152
Lindal, G. F., Lyons, J. R., Sweetnam, D. N., et al. 1987, JGR, 92, 14987
Moreno, R., Lellouch, E., Lara, L. M., et al. 2012, Icarus, 221, 753
Moses, J. I. 2008, LPSC XXXIX conference, 1916
Orton, G. S., Lacy, J. H., Achtermann, J. M., et al. 1992, Icarus, 100, 541
Orton, G. S., Encrenaz, T., Leyrat, C., Puetter, R., & Friedson, A. J. 2007, A&A, 473, L5
Orton, G. S., Fletcher, L. N., Moses, J. I., et al. 2014a, Icarus, 243, 494
Orton, G. S., Moses, J. I., Fletcher, L. N., et al. 2014b, Icarus, 243, 471
Ott, S. 2010, in Astronomical Data Analysis Software and Systems XIX, Proc. Conf., eds. Y. Mizumoto, K.-I. Morita, & M. Ohishi, 434, 139
Pilbratt, G., Riedinger, J. R., Passvogel, T., et al. 2010, A&A, 518, L1
Poglitsch, A., Waelkens, C., Geis, N., et al. 2010, A&A, 518, L2
PACS Observers Manual 2010, http://Herschel.esac.esa.int/Docs/PACS/pdf/pacs_om.pdf
Sromovsky, L. A., Fry, P. A., & Kim, J. H. 2011, Icarus, 215, 292
Sromovsky, L. A., Fry, P. M., Hammel, H. B., et al. 2012, Icarus, 220, 694
Sromovsky, L. A., Karkoschka, E., Fry, P. M., et al. 2014, Icarus, 238, 137
Swinyard, B. M., Polehampton, E. T., Hopwood, R., et al. 2014, MNRAS, 440, 3658
Yelle, R. V., McConnell, J. C., & Strobel, D. F. 1989, Icarus, 77, 439